CONTROLLING ELECTROMAGNETIC FIELDS IN THE TERAHERTZ WINDOW WITH METAL-DIELECTRIC FREQUENCY-SELECTIVE RING RESONATORS

Cosmin Coman[1], Ana Bărar[2], Doina Mănăilă-Maximean[3]

We report theoretical investigations on a modified split ring resonator metasurface architecture, designed to operate in the THz regime. The spectral response of the metasurface is evaluated as a function of variations in the values of the internal ring radius size and linear input polarization state, in terms of reflection, absorption and induced phase, for gold- and copper-polyamide configurations. The plasmonic behavior of the surface is evaluated by means of electric field maps taken at frequencies corresponding to the highest resonance peaks.

Keywords: Terahertz optics, polarization optics, artificial materials, frequency-selective surfaces.

1. Introduction

Metasurfaces [1] are two-dimensional artificial materials that have shown exceptional electromagnetic field interaction capabilities, with a multitude of applications in polarization control [2], wavefront control [3], electromagnetic cloaking [4, 5], generalized reflection and refraction [6, 7]. The interaction mechanism takes place through resonant excitation of surface plasmons [8], which represent collective oscillations of the material regions rather than the individual atoms composing the individual materials. From a construction point of view, the surface plasmons are known as a meta-atom or a meta-cell, the term 'meta' implying the existence of resonances beyond those exhibited by the individual atoms of the interface [9]. The response of the interface is strongly based on the geometry of the surface elements, their relative size, as well as the materials used for their construction. Opposite from diffractive surfaces and photonic crystals, which use an optical path length $D \geq \lambda_0$, where λ_0 represents the working wavelength for continuous-wave applications and the central wavelength for pulse-based applications, metasurfaces obey the strict relation $D \leq \lambda_0/2$. This implies that the sizes of the resonating metastructure units varies roughly between $\lambda_0/10$ and $\lambda_0/3$, depending on the envisioned architecture and associated symmetries. In terms of materials, depending on the spectral window and desired application a series of metal-dielectric [10], semiconductor-dielectric [11] and all-dielectric [12] configurations were used. Some of the materials used can exhibit various piezoelectric capabilities [13], as well as thermal expansion, resulting in externally-addressable responsive architectures. Some architectures, however, do not exhibit full-phase control of the field, a downside which can by bypassed by using external layers of phase controlling coatings. The materials envisioned for the layers can be appropriately-oriented liquid crystal composites, that influence the scattering coefficient [14], input polarization [15]. Also, when mixed with electrically- or magnetically-addressable nanoparticles [16, 17], the critical value of the fields needed to activate the layer are considerably improved [18]. Asymmetric architectures are sensitive to the input polarization, and may exhibit chirality, anisotropy and nonlinear effects, their behavior falling under extended bianisotropic models [19]. A special type of application is represented by electromagnetic

[1]Student, Faculty of Mechanics and Mechatronics, University POLITEHNICA of Bucharest, Bucharest, Romania
[2]Lecturer, Faculty of Electronics, Telecommunications and Information Technology, University POLITEHNICA of Bucharest , Romania, e-mail :ana.barar@upb.ro
[3]Professor, Faculty of Applied Sciences, University POLITEHNICA of Bucharest, Romania

field absorbers, which are typically used and high-power laser systems [20]. Typically, ideal absorption is considered when the full energy of the incoming field is transferred to the surface plasmon oscillation, and either radiated back as heat or converted into low-value surface currents. However, some applications demand the input field is attenuated rather than fully absorbed, with a spectral response which is more pronounced at certain working wavelengths. Such absorbers have been used to highlight phenomena such as giant magnetic resistance [21].

In this paper, we report simulations on a metal-polymer metasurface designed to serve as a variable attenuator in the 2-5 terahertz band. This spectral window is of particular interest for LIDAR and defense applications. The structure is symmetric and uses readily-available materials, which brings the advantage of low production cost. The symmetry of the design ensures smooth transition in the spectral responses of both reflection and attenuation. The absorption peaks can be controlled by means of element sizes, either through construction or through thermal dilation. The scalability of the architecture ensures a similar behavior when shifting towards the mid-infrared and optic spectral windows.

2. **Architecture and simulation conditions**

All configurations and simulations were performed in COMSOL Multiphysics, with the help of the radio frequency (RF) module. The module implements a discretized version of the Helmholtz equation on a finite element mesh, composed of triangles, for an input electromagnetic plane wave of a given frequency. The connfiguration of the field parameters, as well as the Fresnel coefficients are given as a function of the resolution of the mesh, input frequency, polarization and angle of incidence. The unit cell of the metasurface is composed of a metallic ring-like structure with corner symmetry, having an inner radius r_1 and an outer radius r_2. Parallel to the Ox and Oy axes, the ring shape exhibits two asymmetric linear protuberances, with lengths d_1, d_2, and corresponding thicknesses w_1, w_2. Symmetry of the shape is preserved by keeping the size values equal for both protuberances. The height of all components is h_m, and the whole architecture is placed on a square polyamide substrate with lateral dimension a, and height h_{sb}. The inferior side of the polyamide substrate is coated in a complete metallic layer having thickness h_{mb}. for the reference configuration, the dimensions are $a = 36\mu m$, $r_1 = 4\mu m$, $r_2 = 7\mu m$, $d_1 = 6\mu m$, $d_2 = 2\mu m$, $h_m = 0.2\mu m$, $w_1 = w_2 = 1\mu m$, $h_{sb} = 8\mu m$, $h_{mb} = 0.5\mu m$. A schematic view of the architecture, together with the associated geometric parameters is presented in Figure 1.

From a materials point of view, we have considered copper with electric conductivity $\sigma_{Cu} = 5.99 \cdot 10^7$ and gold with electric conductivity $\sigma_{Au} = 4.1 \cdot 10^7$ S/m as the metallic parts of the architecture, and we have performed simulations separately for each material used. For the substrate, we used polyamide with $\varepsilon_{pm} = 2.88 - i \cdot 0.09$, $\mu_{pm} = 1$ and $\sigma_{pm} = 1$, where $i^2 = -1$, regardless of the metallic components under study, due to its transparency in the chosen terahertz band. Due to the periodicity of the structure, the input port was configured as numeric, with the input field being incident on the interface normal to the interface in the reference configuration. The initial intensity was set to the $W/\mu m^2$ level, in order for the background radiation level to reach negligible values. The polarization of the input beam was set to vertical ($\alpha = 90^\circ$). The solver was set to analyze the full field solution, rather than just the background field, in order to account for stray reflection on the air-metacell and metacell-substrate interfaces. The interference component of these stray reflections was then filtered and rejected out of the full solution.

Regarding simulation conditions, the environment was set to create an interface between an air box and two material boxes. To simulate the material, instead of using extrusion techniques, we created an work plane with a penetration depth equal to the architecture component height. This approach is useful due to the fact that it reduces the degrees of freedom on the element. The periodic structure of the unit cell is simulated by establishing a periodic boundary condition endowed with Floquet periodicity, having a wave number that is inferred from the geometry. The periodic boundary conditions are applied on both Ox and Oy. The back plate of the geometry is considered completely

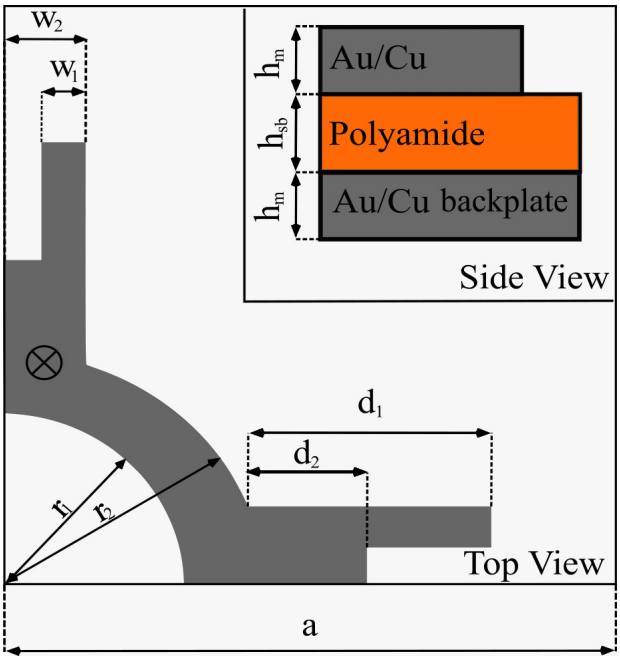

Fig.1. The metasurface cell architecture detailing the geometric parameters and layout. The circled cross represents the incident wave direction.

opaque to the incoming radiation, and therefore an impedance boundary condition was used used. The resulting mesh was set to have a unit triangle lateral size of less than $\lambda_0/20$ for all domains, in order to approach full resolution of the solution. The solver was instructed to solve the Helmholtz equation for the given parameters across the entire mesh, with an iteration feedback loop which is activated if an error of 0.1% with respect to the analytic solution is observed along any element.

3. **Results and discussions**

Taking into account all the above considerations (i.e., architecture, materials and simulation conditions), we obtained a frequency-selective surface in the 2-5 THz band, with distinct spectral responses depending on the different values for both architecture and field parameters.

Gold-polyamide configuration

In the gold ring-polyamide substrate configuration, a significant frequency-selective response is observed in the $2-5$ THz window. The response function is remarkably smooth as a function of frequency, which indicates there are no parasitic surface modes. Such a response is expected due to the symmetry of the architecture. The sensitivity of the response with respect to modifications of architecture parameters was studied by setting fixed values for the internal radius r_1 of the ring, while keeping all other reference parameters constant. The reason for choosing just one architecture parameter to study the sensitivity is the symmetry of the ring and edge rods. The results are shown in Figure 2 and can be discussed as follows:

In the reference architecture configuration in which $r_1 = 4\mu m$, the plasmon response is centered around $f_0 = 3.71$ THz, with a slight asymmetry towards higher frequencies. When scanning the window of interest, the intensity reflection coefficient varies continuously between 0.95, which is typically a mirror-like behavior, to 0.53, which corresponds to a beam splitter configuration. For $f > f_0$, the reflection coefficient rises to 0.75, where it changes monotony. The absorption coefficient closely follows a 'flipped'-monotony function, with values varying from 0.05 at 2 THz, to a

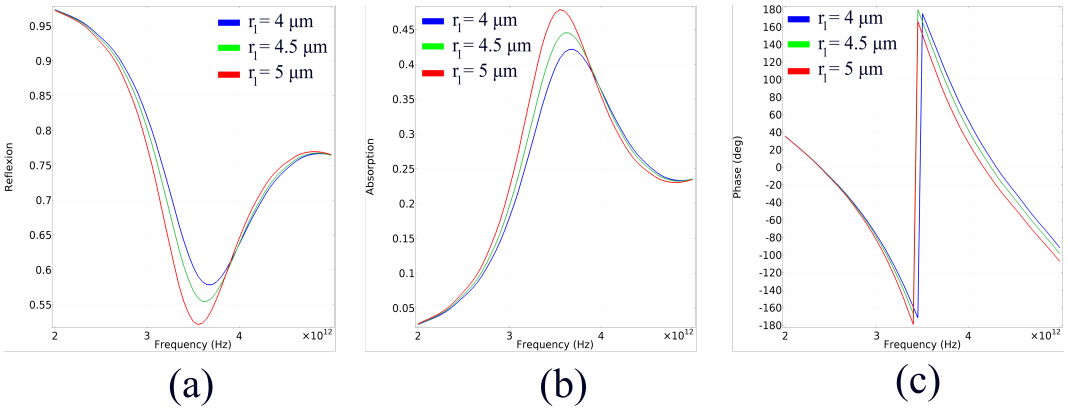

Fig. 2. Frequency-selective response of the gold-polyamide metasurface ar-chitecture under variation of the internal ring radius r_1: (a) reflection; (b) absorp-tion and (c) accumulated phase of the reflected wave.

resonance maximum of 0.47 at f_0, and a decrease to 0.25 at the higher end of the spectrum. The accumulated phase shows a complete 2π range, with a sharp discontinuity from $-\pi$ to $+\pi$ at f_0. When raising the value of r_1, the responses are shifted as follows: the reflection and absorption resonance peak is shifted twoards lower frequencies, with an estimated $f_0 = 3.62$ THz for $r_1 = 4.5\mu m$ and $f_0 = 3.55$ THz for $r_1 = 5\mu m$. The phase map retains the 2π range for all values, and the discontinuity follows the resonance peaks.

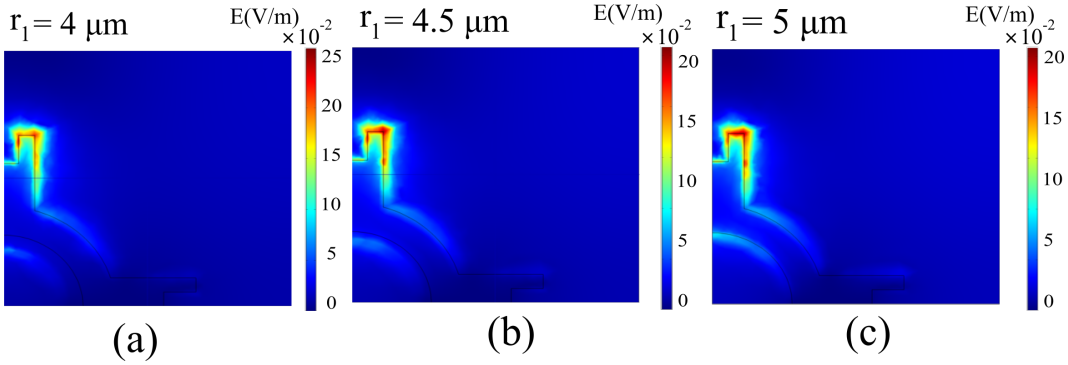

Fig. 3. Electric field distribution at the frequency associated to the highest-valued resonance peak as a function of the variation of the internal ring radius r_1 for the gold-polyamide configuration:
(a) $r_1 = 4\mu m$; (b) $r_1 = 4.5\mu m$; (c) $r_1 = 5\mu m$.

To describe the local effects of the oscillating plasmon, we constructed the electric field maps in the interaction plane for all values of r_1, taken at the resonance peak. As seen in Figure 3, the plasmon is concentrated on the vertical edge of the ring, which is expected for an input vertical polarization.

We also performed a study on the spectral response by varying the linear polarization of the input field through fixed values of 30°, 45° and 60°. For $\alpha = 30°$, the reflection, absorption and phase coefficients can be considered constant across the whole spectrum. For $\alpha = 45°$, the reflection and absorption spectra show a pronounced resonance peak at 3.45 THz, with the values approaching full-range (zero to unity). For $\alpha = 60°$, the resonance peak is diminished and shifted to 3.6 THz. Regarding phase, the configuration $\alpha = 30°$ provides a quasi-constant value, the $\alpha = 45°$

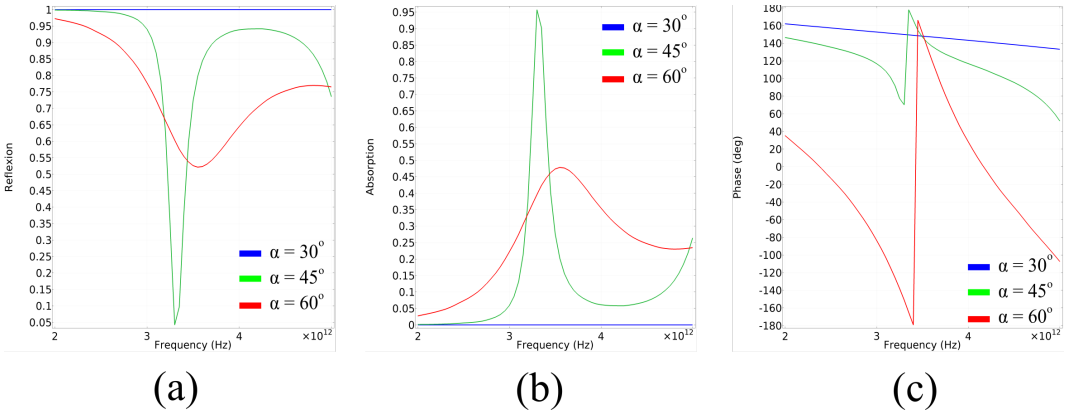

Fig. 4. Frequency-selective response of the gold-polyamide metasurface architecture under variation of the linear input field polarization α:
(a) $\alpha = 0°$; (b) $\alpha = 30°$; (c) $\alpha = 60°$.

configuration offers a relatively-small phase range, in the $100° - 178°$ interval, and the $\alpha = 60°$ configuration offers an almost full 2π range, from $168°$ to $-180°$. The results are presented in Figure 4.

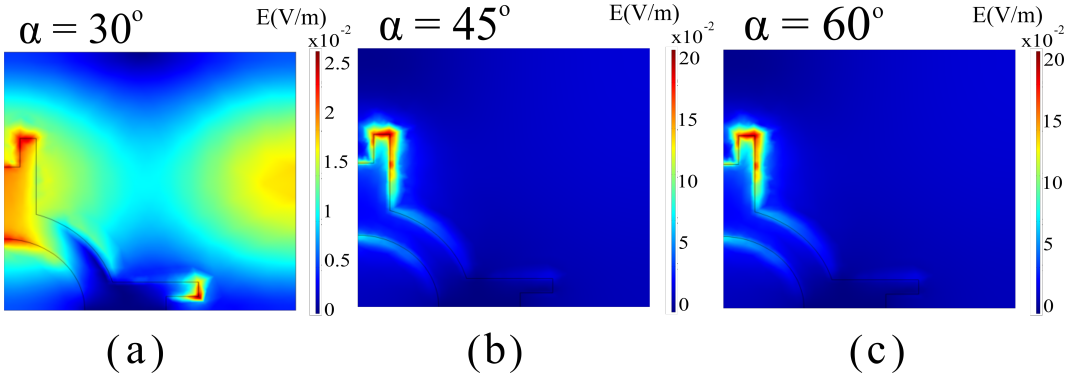

Fig. 5. Electric field distribution at the frequency associated to the highest-valued resonance peak as a function of the input field polarization α for the gold-polyamide configuration: (a) $\alpha = 30°$; (b) $\alpha = 45°$; (c) $\alpha = 60°$.

The study of the response on input polarization is also accompanied by the field distribution map in the interaction plane, at resonance frequency. For $\alpha = 30°$, the resonance frequency was taken at the maximum value of absorption ($f = 5$ THz) field is spread across the interface, with one plasmon located in the upper rod, and the other oscillating outside the ring, on the substrate. The two compensate each other and therefore provide quasi-constant values in reflection and absorption.

Copper-polyamide configuration

To evaluate the response of the architecture comparatively, we have also performed the same simulations for a copper-polyamide metastructure having the same geometry, sizes and input field. The results generate the following discussion:

When cycling through fixed values of the internal ring radius r_1, the reflection, absorption and phase response closely follows that of the gold-polyamide configuration, with resonance peaks obtained at 3.68 THz, 3.56 THz and 3.51 THz for $r_1 = 4\mu m$,$r_1 = 4.5\mu m$ and $r_1 = 5\mu m$ respectively.

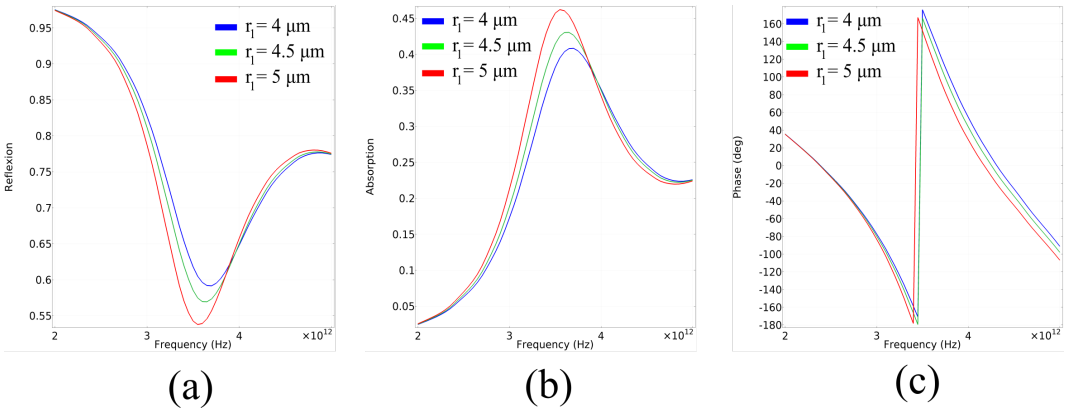

Fig. 6. Frequency-selective response of the copper-polyamide metasurface architecture under variation of the internal ring radius r_1: (a) reflection; (b) ab-sorption and (c) accumulated phase of the reflected wave.

The phase map shows an almost full 2π range for all r_1 configurations, with the sharp discontinuity at resonance. The results are presented in Figure 7.

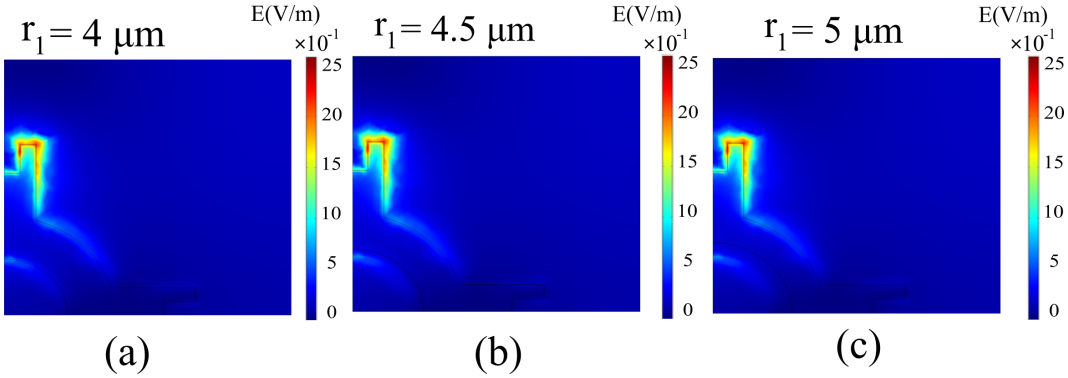

Fig. 7. Electric field distribution at the frequency associated to the highest-valued resonance peak as a function of the variation of the internal ring radius r_1 for the copper-polyamide configuration:
(a) $r_1 = 4\mu m$; (b) $r_1 = 4.5\mu m$; (c) $r_1 = 5\mu m$.

We have also associated the electric field maps in the interface plane at resonance. Just as for the gold-polyamide configuration, the plasmon resonance is located in the top rod of the architecture. The values for the electric field are almost one order of magnitude higher than the ones obtained for the gold-polyamide configuration, which may prove problematic in terms of heat conversion and dissipation inside the structure. The results are presented in Figure 7.

For the polarization-dependent study, we have chosen the same input field polarization as in the gold-polyamide case. The results closely follow the gold-polyamide behavior, with a strong resonance peak observed at $\alpha = 45°$. In the phase response, however, for the $\alpha = 45°$ configuration, the discontinuity exhibits a 2π range, twice as large than the gold-polyamide configuration taken at the same input polarization. The results are presented in Figure 6.

The associated polarization-dependent field maps taken at resonance show that just like in the case of the gold-polyamide configuration, the copper-polyamide metasurface exhibits two plasmonic

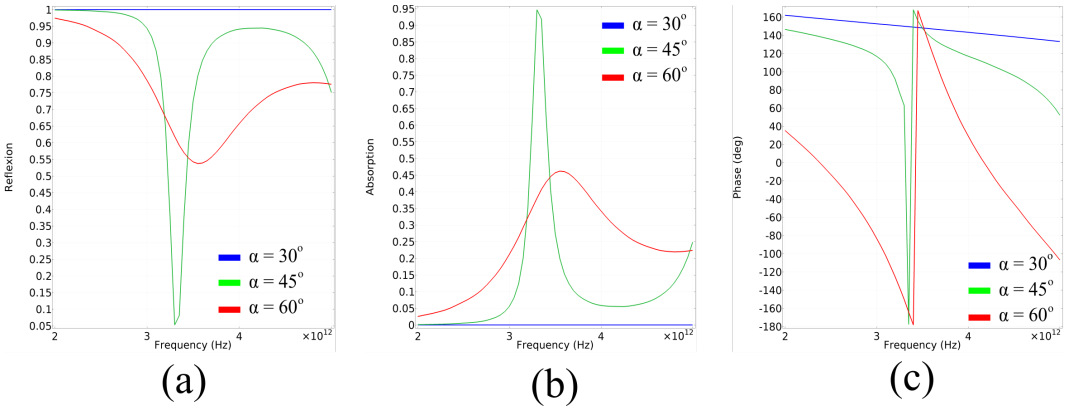

Fig. 8. Frequency-selective response of the copper-polyamide metasurface architecture under variation of the linear input field polarization α: (a) $\alpha = 30°$;(b) $\alpha = 45°$; (c) $\alpha = 60°$.

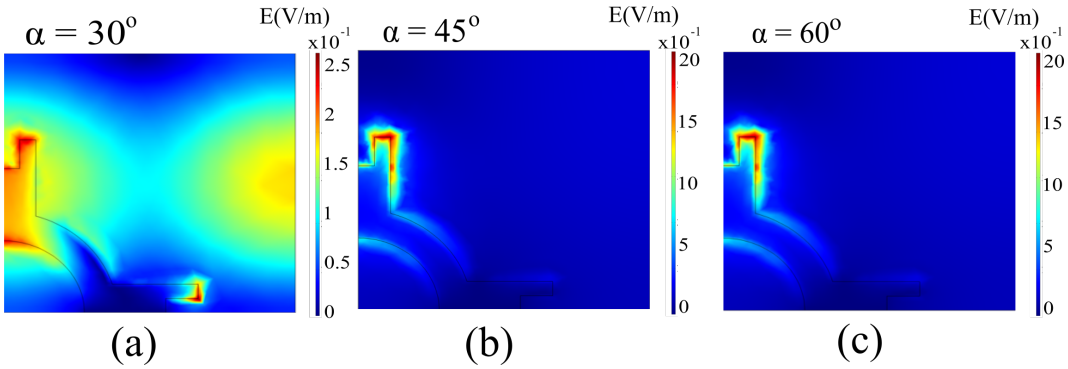

Fig. 9. Electric field distribution at the frequency associated to the highest-valued resonance peak as a function of the input field polarization α for the copper-polyamide configuration: (a) $\alpha = 30°$; (b) $\alpha = 45°$; (c) $\alpha = 60°$.

oscillations in the interface plane for $\alpha = 30°$, which morph into a single plasmonic oscillation localized in the top rod of the ring for $\alpha = 45°$ and $\alpha = 60°$.

4. Conclusions

In this paper, we have performed simulations on the spectral response of gold-polyamide and copper-polyamide metasurface architectures to electromagnetic waves in the 2-5 THz window. The metasurfaces exhibit strong frequency-selective properties, with reflection and absorption coefficients that are strongly dependent on element sizes and input polarization angles. Depending on the configuration, the reflection and absorption can exhibit full range at the resonance peak, as well as full-phase responsiveness in the reflected wave. These properties make the configurations ideal for use in the construction of terahertz mirrors, filters, attenuators and field controllers.

Acknowledgements

We wish to thank O. Dănilă for fruitful discussions and for corrections on the manuscript.

REFERENCES

[1] V. G. Veselago. The electrodynamics of substances with simultaneously negative values of ε and μ. *Soviet Physics Uspekhi*, 10(509), 1968.

[2] M. V. Gorkunov, M. V. Lapine, and S. A. Tretyakov. Methods of crystal optics for studying electromagnetic phenomena in metamaterials: review. *Crystallography Rep.*, 51:1048–1062, 2006.

[3] J. B. Pendry. Negative refraction makes a perfect lens. *Physical Review Letters*, 85(3966), 2000.

[4] U. Leonhardt. Optical conformal mapping. *Science*, 312(5781), 2006.

[5] D. Schurig, J. J. Mock, B. J. Justice, S. A. Cummer, J. B. Pendry, A. F. Starr, and D. R. Smith. Metamaterial electromagnetic cloak at microwave frequencies. *Science*, 314(5801), 2006.

[6] N. Yu, P. Genevet, M. A. Kats, F. Aieta, J. P. Tetienne, F. Capasso, and Z. Gaburro. Light propagation with phase discontinuities: generalized laws of reflection and refraction. *Science*, 334(6054), 2011.

[7] O. Dănilă and D. Manaila-Maximean. Bifunctional metamaterials using spatial phase gradient architectures: generalized reflection and refraction considerations. *Materials*, 14(9), 2021.

[8] J. B. Pendry, A. J. Holden, D. J. Robbins, and W. J. Stewart. Magnetism from conductors and enhanced nonlinear phenomena. *IEEE Transactions on Microwave Theory and Techniques*, 47(11), 1999.

[9] W. Cai, U. K. Chettiar, A. V. Kildishev, and V. M. Shalaev. Optical cloaking with metamaterials. *Nature Photonics*, 1:224–227, 2007.

[10] D. R. Smith, W. J. Padilla, D. C. Vier, S. C. Nemat-Nasser, and S. Schultz. Composite medium with simultaneously negative permeability and permittivity. *Physical Review Letters*, 84(18), 2000.

[11] O. Dănilă. Spectroscopic assessment of a simple hybrid Si-Au metasurface-based sensor in the mid-infrared domain. *Journal of Quantitative Spectroscopy and Radiative Transfer*, 254(107209), 2020.

[12] O. Dănilă, D. Mănăilă-Maximean, A. Bărar, and V. A. Loiko. Non-layered gold-silicon and all-silicon frequency-selective metasurfaces for potential mid-infrared sensing applications. *Sensors*, 21(16), 2021.

[13] O. Dănilă. Polyvinylidene fluoride-based metasurface for high-quality active switching and spectrum shaping in the terahertz G-band. *Polymers*, 13(11), 2021.

[14] V. A. Loiko, A. V. Konkolovich, A. A. Miskevich, D. Mănăilă-Maximean, O. Dănilă, V. Cîrcu, and A. Bărar. Optical model to describe coherent transmittance of polymer dispersed liquid crystal film doped with carbon nanotubes. *Journal of Quantitative Spectroscopy and Radiative Transfer*, 245(106892), 2020.

[15] A. Bărar, O. Dănilă, D. Mănăilă-Maximean, and V. A. Loiko. Active spectral absorption control in a tunable liquid crystal/metamaterial structure by polarization plane rotation. In *International Conference on Nanotechnologies and Biomedical engineeering, Springer, Cham.*, 2019.

[16] D. Mănăilă-Maximean, V. Cîrcu, P. Ganea, A. Bărar, O. Dănilă, T. Staicu, V. A. Loiko, A. V. Konkolovich, and A. A. Miskevich. Polymer dispersed liquid crystal films doped with carbon nanoparticles: electric and electro-optical properties. In *Advanced Topics in Optoelectronics, Microelectronics and Nanotechnologies X*, 2020.

[17] D. Mănăilă-Maximean, C. Cîrtoaje, O. Dănilă, and D. Donescu. Novel colloidal system: magnetite-polymer particles/lyotropic liquid crystal under magnetic field. *Journal of magnetism and magnetic materials*, 438:132–137, 2017.

[18] D. Mănăilă-Maximean, O. Dănilă, C. P. Ganea, and P. L. Almeida. Filling in the voids of electrospun hydroxypropyl cellulose network: dielectric investigations. *The European Physical Journal Plus*, 133(4):1–7, 2018.

[19] O. Dănilă, A. Bărar, M. V. Vlădescu, and D. Mănăilă-Maximean. An extended k-surface framework for electromagnetic fields in artificial media. *Materials*, 14(7842), 2021.

[20] R. Dabu. Femtosecond laser pulses amplification in crystals. *Crystals*, 9(7), 2019.

[21] I. Latella and P. Ben-Abdallah. Giant thermal magnetoresistance in plasmonic structures. *Phys. Rev. Lett.*, 118(173902), 2017.